Localization Patterns in Interstitial Space: A Special Property of the Electron Localization Function (ELF)

Reinhard Nesper* and Steffen Wengert

Dedicated to Professor Dr. Sten Andersson on the occasion of his 65th birthday

Abstract: The electron localization function (ELF) is a new descriptor of chemical bonding in real space which has turned out to be enormously powerful. We show here that the ELF also has predictive power. By analysis of the interstitial space, undetected atoms can be recognized by localization patterns in such regions. The importance of this approach is that the correct number of valence electrons is unknown before the calculations. The method was tested for the compounds Ca_4Sb_2O, Ba_3Ge_4X, $Ba_{10}Ge_7O_3$, and for the so-called second SrSi modification, which, according to our analysis, very probably has the composition $Sr_{10}Si_{10}X$. In these cases the positions of the heteroatoms O and X were located and, in the case of X, proposals for a preferred atom type or group are made. Even in cases where the missing atoms are the majority component the approach was quite successful. As an example, the structure of CaH_2 was generated from the known Ca positions by a two-step iterative procedure.

Keywords
electron localization · hydrides · structure elucidation · Zintl anions

Introduction

The techniques of structure determination of chemical ensembles have developed enormously over the last 50 years.[1] Today the geometrical structure of a compound is the most important basis on which to understand and classify its reactivity. While nowadays diffraction methods constitute a most important part of the determination of structure–property relations, other methods like NMR spectroscopy still have great potential and, despite their present significance, may become still more important in future.[2] To date no combined fitting of model parameters to both diffraction and NMR data has been practically possible, although recent theoretical developments allow for substantial progress.[3, 4]

However, in some cases X-ray diffraction methods face nontrivial problems too, even for small unit cells if, for example, super- or noncommensurate structures have to be determined, if twinning or disorder phenomena demand very sophisticated approaches, or if very light atoms have to be determined against heavy scatterers. In the latter case void search methods[5–8] or molecular modeling may supply some help.[9–11] A void search may be performed on a purely geometrical analysis of the structure, while force-field methods can only work successfully if good potential parameters and reliable effective charges are known, conditions that quite frequently cannot be met.

In some cases, important bonding considerations arise from the question of whether all atoms of a structure have been reliably located or not. If this is not the case, chemical arguments may help to settle this question. For example, normal Zintl phases like main group silicides can in general be rationalized by the application of simple bonding concepts based on electron-counting rules.[12] If, however, unusual or unexpected moieties occur it is not always certain whether they really do exist or are just the result of an erroneous structure determination.[13–16] The existence of a geometrical void in such a structure reasonably has to generate suspicion, but it cannot be used as a safe indicator for an overlooked atom or group of atoms. The "free" space may be generated for electronic reasons, for example as a packing space for free electron pairs which are tightly bound to specific atoms, or of more or less free electrons as in electrides, intermetallics, and metals. In the latter case an additional electron volume which is relatively independent of the actual atom distribution has to be considered.

We would like to present here a novel property of the electron localization function (ELF)[17] that may help quite effectively in such difficult situations. The ELF turned out to be an extraordinarily useful electron localization sensor for interstitial space, a property which is especially useful for checking trial structures in problematic cases, as mentioned before.

The ELF can be generated on the basis of quantum mechanical calculations of quite different levels of sophistication, for example extended Hückel, Hartree–Fock, or density functional

[*] Prof. Dr. R. Nesper, Dipl.-Chem. Steffen Wengert
Laboratorium für Anorganische Chemie
Eidgenössische Technische Hochschule, ETH Zentrum
CH-8092 Zürich (Switzerland)
Fax: Int. code +(1)632-1149
email: nesper@inorg.chem.ethz.ch

  0947-6539/97/0306-0985 $ 17.50+.50/0

methods. It has been shown that the ELF is able to display chemical bonding in its different occurrences very clearly, distinctly, and fairly comprehensively. There have been quantitative and qualitative investigations of electronic structures of molecules,[18] clusters,[19] ring systems,[20] semiconductors,[21] intermetallic compounds, and pure metals[22] as well as of surfaces and surface reconstructions,[23] which show impressively that a novel descriptor and measure of chemical bonding is gained with the ELF.[24, 25]

Here we should point out that the ELF enables the visualization of patterns in interstitial spaces in such regions which can hardly be associated with single atoms. Such patterns, which indicate weakly bound but still spatially localized electrons, are in many cases indicative of overlooked atoms and thus may be of considerable importance for checking the correctness of a structure. We would like to present this sensor function of the ELF by means of four examples, namely Ca_4Sb_2O,[26] Ba_3Ge_4X,[27] $Ba_{10}Ge_7O_3$,[28] and CaH_2.[29, 30] Furthermore we will try to predict missing atoms in hitherto accepted structures, for example, in the so-called second modification of SrSi.[31] The starting point of our investigations was in fact the theoretical treatment of this unusual modification, which led us to the detection of the phenomenon we would like to present here. To back up our findings concerning the ELF on the basis of theoretical LMTO band structure calculations[32] we analyzed in the same way Zintl phases that have proved to contain light heteroatoms in addition to Zintl anions and heavier cations.

Results and Discussion

Location of missing atoms in Ca_4Sb_2O: Compound Ca_4Sb_2O[26] was first described as binary calcium antimonide Ca_2Sb,[35] an assertion corrected shortly after by the authors themselves. The structure contains isolated Sb^{3-} anions and thus can only meet the electronic structure of a semiconducting valence compound as experimentally confirmed if another X^{2-} entity is present to accumulate the excess electrons from the calcium. The additional anion was identified as O^{2-} coordinated octahedrally by six Ca atoms (Figure 1a).

Surprisingly, the calculation of the ELF for Ca_4Sb_2 (based on a LMTO calculation without the O atom![37, 36]) generates one and only one additional localization region, which lies at the center of the Ca octahedron (Figure 1b, white area). After introduction of the O atom (and six more valence electrons) into the calculation, an ELF is yielded which clearly displays the O atom with its core regions (white shell, Figure 1c). It is remarkable that despite the use of the different electron counts, namely those for Ca_4Sb_2 ($8+10e^-$) and for Ca_4Sb_2O ($8+10+6e^-$), similar localization patterns are found in the two cases.

As expected from the conception of Zintl, Klemm, and Busmann (ZKB)[12] the density of states (DOS) of Ca_4Sb_2O shows a clear band gap of about 2 eV in the region of the Fermi energy while the hypothetical Ca_2Sb turns out to be metallic (Figure 2). The DOS of Ca_4Sb_2O below the Fermi energy may be divided into three separate energy ranges, namely the Sb s, the O p, and the Sb p regions (the O s states are much lower in energy and were treated in the LMTO calculation as a core function). Thus, within the ZKB picture we can formally speak of Ca_4Sb_2O as

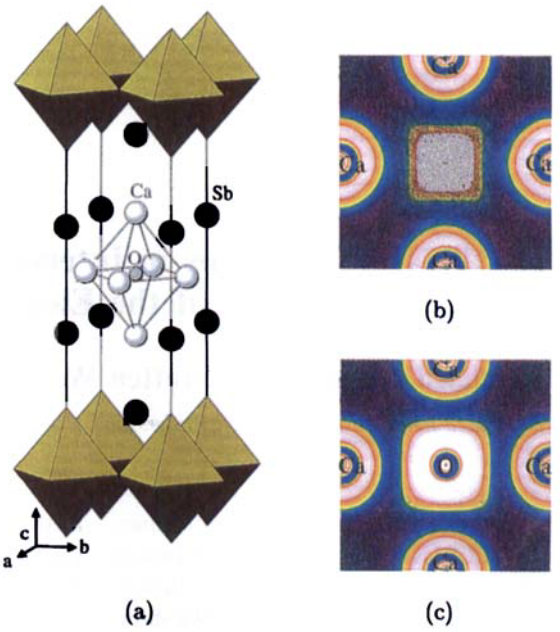

Figure 1. a) Perspective view of the structure of Ca_4Sb_2O; b) ELF distribution in a two-dimensional section through the base of the Ca_6 octahedron (ref. [36]), calculated without O atom; c) calculated with O atom.

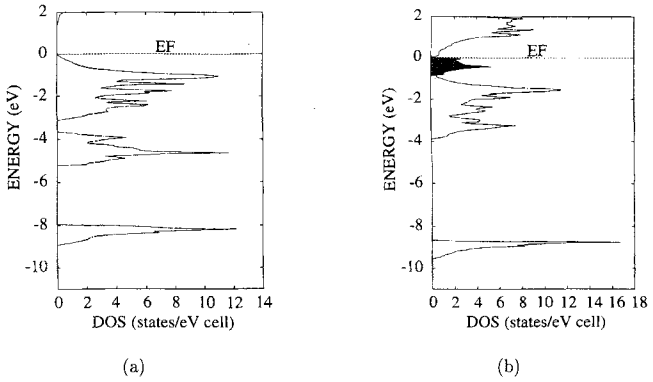

Figure 2. Density of states (DOS) based on LMTO calculations: a) Ca_4Sb_2O and b) Ca_2Sb.

$(Ca^{2+})_4(Sb^{3-})_2(O^{2-})$. On the other hand, the DOS of Ca_2Sb shows, as well as the comparable Sb s and Sb p regions, an additional peak between the virtual metallic and the occupied Sb region (Figure 2, grey area). The corresponding states contain the two excess electrons remaining after the occupation of Sb states. Analysed by means of partial density (within the energy range marked in grey) these states turn out to be mainly localized in the centers of the Ca_6 octahedra (Figure 3), exactly

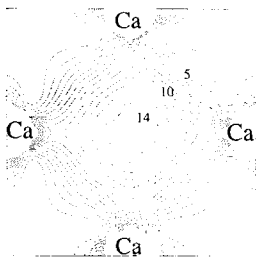

Figure 3. Partial density of Ca_2Sb in the energy range $-1\ eV < E < E_f$. Two-dimensional section in the (001) plane through the base of the Ca_6 octahedron. The contour values are given in ($e^{-1}au^{-3}$).

0947-6539/97/0306-0986 $ 17.50+.50/0 Chem. Eur. J. 1997, 3, No. 6

those regions where the ELF distribution shows an extraordinary maximum. Thus the ELF just marks localized metallic states, the so-called *cage orbitals*,[16] which act as HOMOs in the sense of a frontier orbital picture of the reaction with oxygen.[38, 39] This may explain why oxygen is built in exactly at these positions in the centers of the Ca_6 octahedra.

Location of X/O in Ba_3Ge_4X and $Ba_{10}Ge_{10}O_3$: Quite recently von Schnering et al. synthesized derivatives of barium germanides which contain Ba_6X octahedra and typical Zintl anions of germanium. In Ba_3Ge_4X[27] there are Ge_4^{4-} tetrahedrons, and in $Ba_{10}Ge_{10}O_3$[28] planar Ge_6^{10-} rings besides isolated Si^{4-} units occur (Figures 4a and 5a). Both structures can be viewed as a framework of corner-shared Ba_6 octahedra with the corresponding Zintl anions embedded in the remaining voids. The ELF distributions (based on LMTO calculations[40]) without the heteroatoms X show localization patterns which are exactly and exclusively at those positions that are occupied by X. Figures 4b–c and 5b–c display corresponding ELF sections through the Ba_6 octahedra without and with heteroatoms (X = O) for Ba_3Ge_4X and $Ba_{10}Ge_7O_3$, respectively. The ELF denotes the sites of the heteroatoms quite convincingly. According to electron counting rules, X^{2-} units of small groups such as O^{2-}, C_2^{2-}, NH^{2-}, are expected.[41]

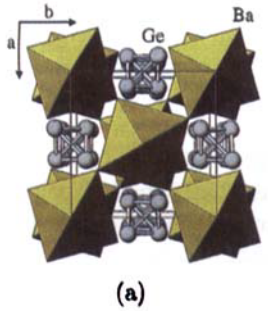

(a)

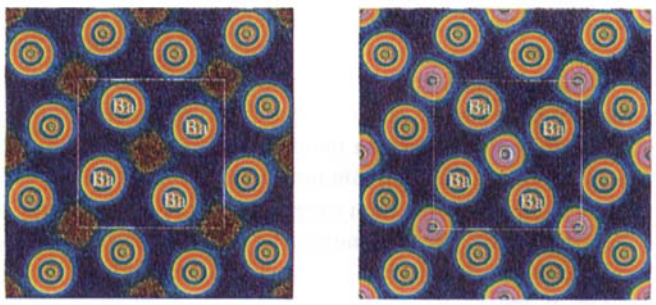

(b) (c)

Figure 4. a) Perspective view of the structure of Ba_3Ge_4X; b) ELF sections through the base of the Ba_6 octahedra without and c) with heteroatom (X = O).

Location of hydride positions: We believe that a related test for a hydride structure is of special interest and importance, because in general, hydrides present a problem for X-ray crystallography. Quite frequently, hydride samples are microcrystalline and thus single-crystal investigations cannot be performed. Furthermore, hydride positions may not be found by X-ray analysis

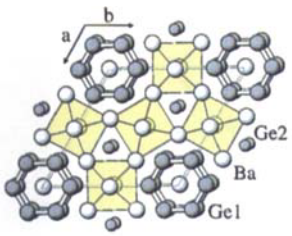

(a)

(b) (c)

Figure 5. a) Perspective view of the structure of $Ba_{10}Ge_7O_3$; b) ELF sections through the base of the Ba_6 octahedra without and c) with heteroatom (X = O).

because of the small scattering factor of H. In some cases electronic cluster concepts may favor interstitial H atoms as in $Nb_6I_{11}H$[42] or in $Th_6Br_{17}H_5$[43] at certain well-defined positions. Still there may be considerable ambiguity about the H positions: in $Nb_6I_{11}H$ there is a hydrogen atom in the center of the Nb_6 cluster; however, in $Th_6Br_{17}H_5$ only five of the six faces of the Th_6 octahedron can be occupied, giving rise to statistical distribution for the overall crystal structure.

We chose the structure of CaH_2 as an example and performed the analysis as follows: band structure and subsequent ELF calculations were performed starting with the pure Ca substructure to follow a typical development of a hydride structure determination.[44] Figures 6b–d display a section of the structure that contains all crystallographically independent positions Ca, H1, and H2. In Figure 6b the ELF is shown for the pure Ca substructure, which means without electron acceptors H. The valence electron count per formula unit is two. There is a weak but significant localization (typical for intermetallic compounds and metals) that includes the H2 position. If now one H atom per formula unit (three valence electrons) is added and located at that site, a new localization spot that coincides with the position of H1 becomes clearly visible (Figure 6c). Actually this region is already distinct in the ELF for the pure Ca substructure, but the localization is not much higher than for a neighboring position unoccupied by H in the real structure. It may, however, be a potential interstitial position that might, for example, be used as a jump position if H^- ion mobility occurred. These two weaker localization regions can be clearly distinguished after introduction of the first H site (H2). However, a choice between the first not quite correct structure determination of CaH_2[29] and the second one[30] cannot easily be made by an ELF analysis because the differences, which concern only the position H2, are quite small ($\Delta \approx 30$ pm). Finally, the ELF of the complete structure (Figure 6d) reveals the ionic character of this hydride beautifully: there are only low ELF minima (green to blue) between the atoms. Despite that, a significant polarization is visible, especially of the hydride ions but also of

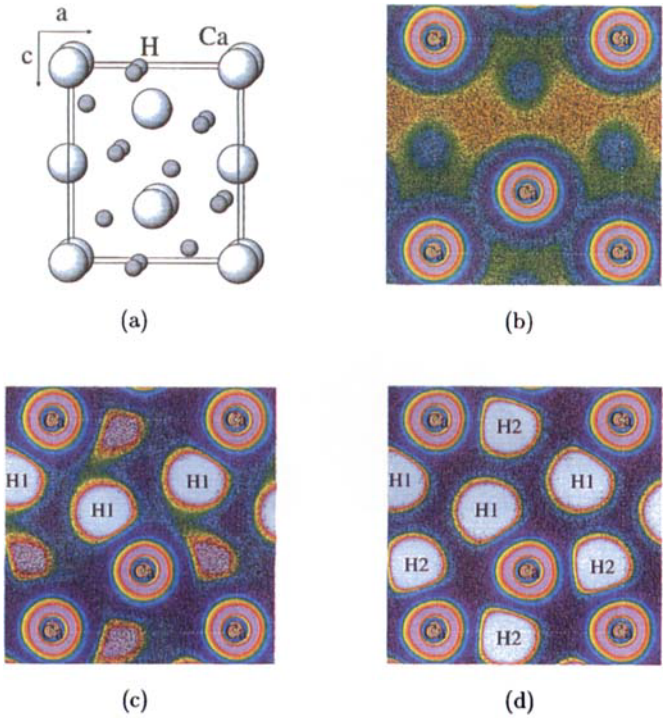

Figure 6. a) Perspective view of the structure of CaH_2; ELF sections in a (010) plane. b) LMTO calculation without and c) with one H position (H1) and d) with all H atoms (ref. [44]).

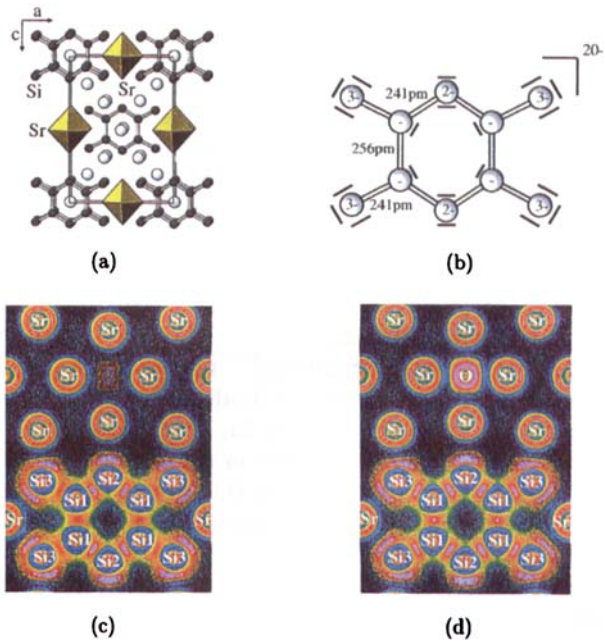

Figure 7. a) Perspective view of the structure of "SrSi"; ELF distribution in perpendicular sections [010]. b) SrSi; c) $Sr_{10}Si_{10}O$.

the Ca^{2+} cations, which induces deviations from the spherical symmetry. The considerable deviation of the polarized ions from spherical symmetry may give rise to the low triclinic symmetry of the whole structure, but allowing for relatively short distances and high density.

Structure of the second modification of "SrSi": The so-called second modification of SrSi (Figure 7a), which was never confirmed experimentally, contains a very interesting Zintl anion, a planar $[Si_{10}]^{20-}$[31] with quite peculiar bond distance differences. With respect to the ZKB concept, one would expect a formal charge distribution for Si_{10} like that depicted in Figure 7b. However, the bond distances Si1–Si1 (256 pm) are so much longer than the other two (Si1–Si2 241 pm, Si1–Si3 241 pm) that a simple singly bonded system with an overall charge of $q = -20$ seems quite suspect. A closer look at the cation structure shows that the Sr atoms form an empty distorted octahedron. The ELF treatment[45] reveals a localization pattern consistent with the assumption of single bonds between Si1 and Si2 and a weak bond between Si1 and Si1. The other short bond, Si1–Si3, however, unexpectedly has only the localization pattern of a weak bond and not the white spot which was expected from valence rules, the ZKB concept, and bond length/bond strength considerations. Even more surprising is a large localization region in the center of the Sr_6 octahedron (upper middle in Figure 7b). The four surrounding atoms and two above and below that plane generate the octahedron, which, incidentally, shows a remarkable contraction compared with the neighboring rectangles. Too high an accumulation of charge on the Zintl anion could lead to a charge back-transfer to strontium and formation of an Sr-centered cage orbital.[13] In this case, SrSi would belong to the class of electrides on the one hand and to that of the metal cluster compounds on the other.

Another explanation, however, seems more reasonable to us, namely that the center of the Sr octahedron is occupied by a light heteroatom, for example by oxygen. The corresponding distances (4×245, 2×285 pm, $\bar{d} = 258$ pm) fit well with this hypothesis. Distances in SrO (rocksalt type, 6×257 pm[46]) or $SrTiO_3$ (perowskite, 12×276 pm[47]) compare well if in the latter case the higher coordination number of Sr is taken into account. The presence of a heteroatom would also explain the failed attempts to synthesize this "SrSi" modification from especially purified elements.[48]

Both extended Hückel[49, 50] and LMTO band structure calculations for $Sr_{10}Si_{10}$ ("SrSi") and $Sr_{10}Si_{10}O$ reveal a band crossing at the Fermi level, indicating metallic conductivity;[51] we therefore believe that the corresponding real compounds would not have a band gap (Figure 8). This means that there is no preferred valence electron number to be extracted from the density of states (DOS) distribution. This, however, allows for small heteroatoms other than oxygen, such as F, N, or even C.

For the binary "SrSi", unusual Sr contributions to a few bands below the Fermi level occur, which diminish after introduction of the heteroatom (O). A complete filling of these bands, which arise from the antibonding π^* states of the Si_{10} unit corresponding to the Lewis formulation in Figure 7b, is not obtained, independent of the type of the above-mentioned heteroatoms. In all cases a weak π-bonding character remains in the Si_{10} anion; this reduces the effective lone pair contribution to the electronic structure. The π states perpendicular to the ring plane overlap between the ecliptically stacked adjacent Si_{10} units. This gives rise to a σ-like weak bonding interaction along the stacks, which serves as an adaptable electron sink. In the band structure one finds considerable dispersion of the related π bands (see Figure 8). This situation was observed quite recently for a number of binary and ternary silicides that contain

0947-6539/97/0306-0988 $ 17.50+.50/0 Chem. Eur. J. 1997, 3, No. 6

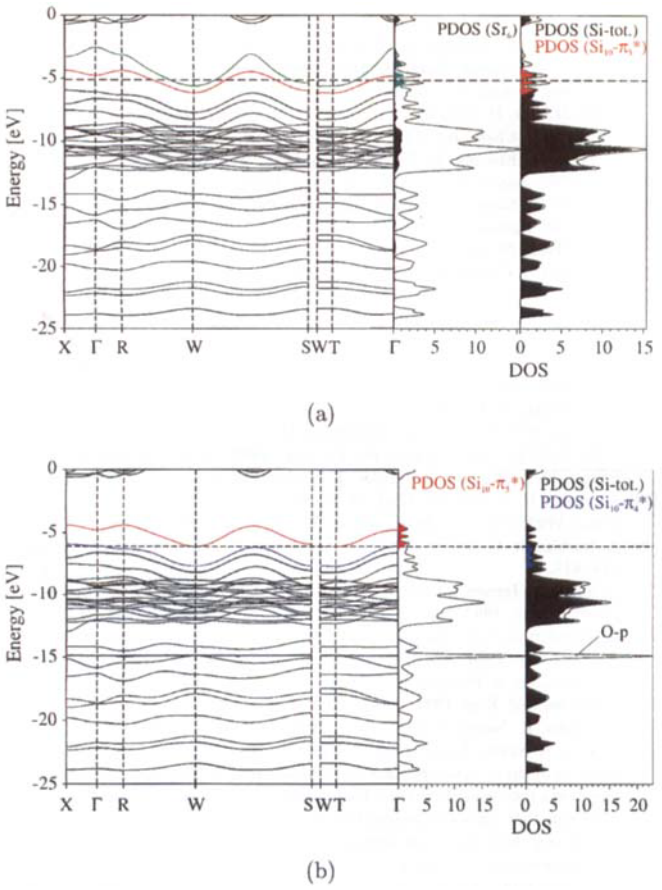

Figure 8. EHMO band structure and DOS curves of a) SrSi, b) $Sr_{10}Si_{10}O$.

planar Si_n units stacked ecliptically as in the compound discussed here.[15] These interactions are found both in extended Hückel and in LMTO calculations. In addition, the more precise first principle LMTO investigations reveal that close to the Fermi level σ^* and π^* contributions are present; this means that small changes of the valence electron number will change both σ and π bonding (Figure 7c,d). Thus competition of σ^*, π^*, and free electron pair states generates a quite complex electronic structure close to E_F that does not allow for a clear definition of a preferred valence electron number. Without this collective bonding effect, $Sr_{10}Si_{10}O$ would clearly be a semiconductor (Figure 8).

Based on a corresponding LMTO band structure for $Sr_{10}Si_{10}O$, the ELF shows a surprisingly reasonable localization pattern under this model situation (Figure 7c). We would like to emphasize that it was not obvious from the beginning that a removal of two electrons from the $Sr_{10}Si_{10}$ structure would generate a near-normal bonding pattern with lone pairs and weaker and stronger bonds with expected qualitative ratios of relatively high localization regions.

The geometrical analysis of the structure shows that another void is present, enclosed by the semicircle Si 3-Si 1-Si 1-Si 3 close to the Si 1–Si 1 bond. There are two of these positions per Si_{10} unit, and consequently two hydrogen atoms could be present. However, each of them would be engaged in a five-center two-electron bond (Si 3, Si 1, Si 1, Si 3, H), and this does not seem to be very probable, because not even μ_2-bridging H atoms have ever been observed in hitherto known silanes. There is only spectroscopic[52] and theoretical evidence for such bonding situations for small molecules like Si_2H_2.[4, 53] Considering the possible hydrogen content in the compound, the compositions $Sr_4(Sr_6O)Si_{10}H_2$ or $Sr_{10}Si_{10}H_2$ could occur, both of which would be metals according to the calculated band structures and thus not preferred against the pure suboxide. Furthermore, there is no particular additional localization in the regions in question separable from the localization centers which have to be assigned to the Si_{10} cluster. Finally, the localization maximum between the Si 1 atoms does not deviate from the interatomic vectors towards the possible H position. Thus, we believe that there is no hydrogen present in this compound, but only oxygen, according to the formula $Sr_{10}Si_{10}O$. Hence, the Zintl anion Si_{10}^{18-} has to be interpreted as a weakly bonded dimer of two Si_5^{9-} chain sections.

Identification of oxygen in a silicide: A check of our own recently found new silicides with the ELF analysis revealed straightforwardly that we have overlooked an oxygen atom in the structure of $Sr_{11}Mg_2Si_{10}$ (refs. [54,55]; Figure 9a). Out of a large number of silicides with planar Si_n anions, this was one of the very few for which no π-bond contribution was expected according to the formulation $[Sr^{2+}]_{11}[Mg^{2+}]_2[Si_8^{18-}][Si^{4-}]_2$. The special Zintl anion here is the all-*trans* zigzag chain section Si_8. This formal Zintl Klemm-type description implied a normal Zintl compound with a purely σ-bonded chain system. This match with the normal valence rules and the knowledge that there is no energy gain for silicon from the formation of π bonds instead of σ bonds[56] dissuaded us from checking this compound immediately, although a fairly low yield in the synthesis indicated that better synthesis conditions had to be evaluated.

The ELF treatment for this compound shows a marked localization region inside an "empty" Sr_6 unit with the form of a distorted octahedron (Figure 9b,c). Reaction of stoichiometric amounts of SrO, Sr, Mg, and Si gave the pure phase $Sr_5(Sr_6O)Mg_2Si_{10}$ within a few percent. Supporting single-crystal investigations confirmed the full oxygen occupancy of the central site in the Sr_6 octahedron.[55] This not only demonstrates

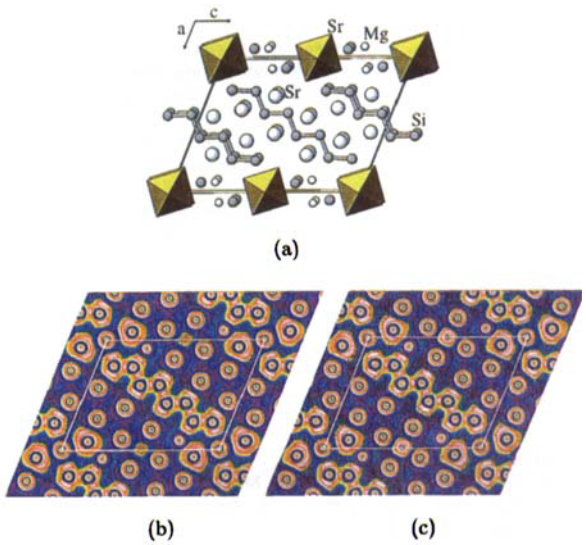

Figure 9. a) Perspective view of the structure of $Sr_{11}Mg_2Si_{10}O$; ELF distribution in perpendicular sections [010]. b) $Sr_{11}Mg_2Si_{10}$; c) $Sr_{11}Mg_2Si_{10}O$.

that such ELF analyses do have a reasonable predictive and analytical character, but also that heteroatom inclusions like O and N and possibly C, B, or F, too, are not impurities but structurally important entities that do form inverse cationic complexes M_mX^{n+}. Such complex cations, which may be found everywhere in oxides and thus may at first sight be considered as trivial descriptions, obtain a new meaning in Zintl phases with formally highly charged anions, because they occur here as separable or isolated units. Further, such entities are also highly charged large cations, a combination that is quite rare in chemistry. Interestingly, just this kind of cation is needed to separate and stabilize very sensitive and highly reducing Zintl anions with large formal charges. It need not be stressed that such entities have been sought for a long time, ever since attempts were first made to dissolve Zintl anions in polar solvents. Up to now success has only been achieved in cases where the Zintl anions had fairly low formal charges. The features we find in our ELF map directly support these findings.

Conclusion

We consider that the ELF is able to describe chemical bonding in molecules, clusters, and extended structures so well that even information about missing atoms can easily be extrapolated from the function. It should be emphasized that in cases like CaH_2 even positions for the majority component atoms may be found, as we have shown. In case of suspect structures, we propose to calculate the ELF for the known (partial) structure (if necessary applying different valence electron numbers, for example for EH calculations) to yield an impression as to whether the structural capability of localizing valence electrons is reasonable.

Acknowledgments: We are grateful for the support of the Swiss National Science Foundation and the ETH (project nos. 20-43-228-95 and 0-20-288-96, respectively) and the supercomputing project C^4. We also thank Prof. Dr. H. G. von Schnering for supplying structural data prior to publication.

Received: January 20, 1997 [F580]

[1] a) J. Karle, *Angew. Chem.* **1986**, *98*, 611; *Angew. Chem. Int. Ed. Engl.* **1986**, *25*, 614; b) H. Hauptmann, *ibid.* **1986**, *98*, 600 and **1986**, *25*, 603.
[2] R. R. Ernst, *Angew. Chem.* **1992**, *104*, 817; *Angew. Chem. Int. Ed. Engl.* **1992**, *104*, 805.
[3] a) W. Kutzelnigg, *Isr. J. Chem.* **1980**, *19*, 193; b) W. Kutzelnigg, U. Fleischer, W. Schindler, *NMR Basic Principles and Progress, Vol. 23*, Springer, Berlin, **1990**.
[4] Y. Apeloig, M. Karni, T. Müller, in *Organosilicon Chemistry, Vol. II, From Molecules to Materials* (Eds.: N. Auner, P. Weis), VCH, Weinheim, **1995**, pp. 263 ff.
[5] P. Niggli, *Z. Kristallogr.* **1928**, *68*, 404.
[6] F. Laves, *Z. Kristallogr.* **1931**, *78*, 208.
[7] R. Nesper, *Angew. Chem.* **1991**, *103*, 805; *Angew. Chem. Int. Ed. Engl.* **1991**, *30*, 789.
[8] B. Bitterli, Diplomarbeit, ETH Zürich, **1993**.
[9] H. G. von Schnering, Habilitationsschrift, Universität Münster, **1963**.
[10] U. Duffe, *Programm zur Lokalisierung von Protonenpositionen in Kristallstrukturen/Program for the localization of protons in crystal structures*, Universität Münster, **1972**.
[11] R. Nesper, Dissertation, Universtät Münster, **1978**.
[12] E. Zintl, *Angew. Chem.* **1939**, *52*, 1; E. Zintl, G. Brauer, *Z. Phys. Chem.* **1933**, *B20*, 245; E. Zintl, W. Dullenkopf, *ibid.* **1931**, *A154*, 1; *ibid.* **1932**, *B16*, 183; W. Klemm, *FIAT Review of German Science/Naturforschung und Medizin in Deutschland* **1939–1946**, *Anorganische Chemie Teil IV*, *26*, 103; W. Klemm, *Trab. Reun. Int. React. Sólidos 3* **1956**, *1*, 447; W. Klemm, *Proc. Chem. Soc. London* **1959**, 329; E. Mooser, W. B. Pearson, *Phys. Rev.* **1956**, *101*, 1608; E. Mooser, W. B. Pearson, in *Progress in Semiconductors, Vol. 5* (Ed.: A. F. Gibson), Heywood, London, York, **1960**, p. 103; W. Klemm, *Festkörperprobleme*, Vieweg, Braunschweig, **1963**; E. Busmann, *Z. Anorg. Allg. Chem.* **1961**, *313*, 90; H. Schäfer, B. Eisenmann, W. Müller, *Angew. Chem.* **1973**, *85*, 742; *Angew. Chem. Int. Ed. Engl.* **1973**, *12*, 694.
[13] H. G. von Schnering, R. Nesper, J. Curda, K.-F. Tebbe, *Angew. Chem.* **1980**, *92*, 1070; *Angew. Chem. Int. Ed. Engl.* **1980**, *19*, 1033; M. C. Böhm, R. Ramirez, R. Nesper, H. G. von Schnering, *Phys. Rev.* **1984**, *B30*, 4870; M. C. Böhm, R. Ramirez, R. Nesper, H. G. von Schnering, *Ber. Bunsenges. Phys. Chem.* **1985**, *89*, 465.
[14] R. Nesper, J. Curda, *Z. Naturforsch.* **1987**, *42b*, 557.
[15] R. Nesper, A. Currao, S. Wengert in *Organosilicon Chemistry Vol. II, From Molecules to Materials* (Eds.: N. Auner, P. Weis), VCH, Weinheim, **1995**, pp. 469 ff.
[16] R. Ramirez, R. Nesper, H. G. von Schnering, M. C. Böhm, *J. Phys. Chem. Solids* **1987**, *48*, 51.
[17] A. D. Becke, N. E. Edgecombe, *J. Chem. Phys.* **1990**, *92*, 5397.
[18] A. Savin, H. J. Flad, J. Flad, H. Preuss, H. G. von Schnering, *Angew. Chem.* **1992**, *104*, 185; *Angew. Chem. Int. Ed. Engl.* **1992**, *31*, 185; D. Seebach, H. M. Bürger, D. A. Plattner, R. Nesper, T. Fässler, *Helv. Chim. Acta* **1993**, *76*, 2581.
[19] A. Savin, H. J. Flad, O. Flad, H. W. Preuss, H. G. von Schnering, *Angew. Chem.* **1992**, *104*, 185; *Angew. Chem. Int. Ed. Engl.* **1992**, *31*, 187.
[20] A. Burkhardt, U. Wedig, H. G. von Schnering, *Z. Anorg. Allg. Chem. C* **1993**, *619*, 437.
[21] A. Savin, O. Jepsen, J. Flad, O. Anderson, H. W. Preuss, H. G. von Schnering, *Angew. Chem.* **1992**, *104*, 186; *Angew. Chem. Int. Ed. Engl.* **1992**, *31*, 187.
[22] U. Häußermann, S. Wengert, P. Hofmann, A. Savin, O. Jepsen, R. Nesper, *Angew. Chem.* **1994**, *106*, 2147; *Angew. Chem. Int. Ed. Engl.* **1994**, *33*, 2069; U. Häußermann, S. Wengert, R. Nesper, *Angew. Chem.* **1994**, *106*, 2151; *Angew. Chem. Int. Ed. Engl.* **1994**, *33*, 2073.
[23] T. Fässler, R. Nesper, *Chem. Eur. J.* **1995**, *1*, 625.
[24] B. Silvi, A. Savin, *Nature* **1994**, *371*, 683.
[25] Savin et al. have developed a new nomenclature for regions with high ELF based on a topological analysis. They classify the ELF maxima into: asynaptic: maximum that cannot be assigned to an atom; monosynaptic: one-centre localization (e.g. lone pair, core region); bisynaptic: two-centre localization (e.g. two-electron-centre bonding); trisynaptic: three-centre localization (e.g. three-centre bonding); A. Savin, B. Silvi, F. Colonna, *Can. J. Chem.* **1996**, *74*, 1088.
[26] B. Eisenmann, H. Limartha, H. Schäfer, H. A. Graf, *Z. Naturforsch.* **1980**, *35*, 1518.
[27] H. G. von Schnering, M. Somer, J. Curda, personal communication.
[28] H. G. von Schnering, U. Bolle, J. Curda, K. Peters, W. Carrillo-Cabrera, M. Somer, M. Schultheiss, U. Wedig, *Angew. Chem.* **1996**, *108*, 1062; *Angew. Chem. Int. Ed. Engl.* **1996**, *35*, 984.
[29] B. Bergsma, B. O. Loopstra, *Acta Crystallogr.* **1962**, *15*, 92.
[30] A. F. Andresen, A. J. Maeland, D. Slotfeld-Ellingsen, *J. Solid-State Chem.* **1977**, *20*, 93.
[31] B. Eisenmann, H. Schäfer, K. Turban, *Z. Naturforsch.* **1974**, *29b*, 464.
[32] TB-LMTO-ASA: Tight-binding linear muffin-tin orbital in the atomic sphere approximation; M. van Schilfgarde, T. A. Paxton, O. Jepsen, O. K. Andersen, G. Krier, Programm TB-LMTO, Max-Planck-Institut für Festkörperforschung, Stuttgart, **1994**, unpublished; the TB-LMTO-ASA calculations are based on the LDA approximation with an exchange-correlation potential due to Barth and Hedin [33]. The radii of the overlapping muffin-tin spheres in the ASA approximation are chosen as described by Jepsen and Andersen [34]. The muffin-tin radii and positions for the required empty spheres (ES) are listed for every compound separately. They are given in atomic units and crystal coordinates, respectively.
[33] U. Barth, L. Hedin, *J. Phys. C* **1972**, *5*, 1629.
[34] O. Jepsen, O. K. Andersen, *Z. Phys B* **1995**, *97*, 35.
[35] B. Eisenmann, H. Schäfer, *Z. Naturforsch.* **1974**, *29b*, 13; C. Harmon, R. Marchand, P. L'Haridon, Y. Laurent, *Acta Crystallogr.* **1974**, *31 B*, 427.
[36] The ELF distributions in the current work are shown in selected sections of the structures considered. The pixel density is based on the electron density and is colored according to the corresponding ELF values. Roughly, the color scale can be viewed as: white: ELF 1.0–0.9, red: ELF 0.9–0.6, green: ELF 0.6–0.4, blue: ELF $\leq$ 0.4. The regions of high ELF values (0.9–1.0) correlate quite well with the presence of bonding, lone pairs and core regions.
[37] Ca_4SbO: 59 irreducible k-points, Ca 1 (2.93), Ca 2 (3.43), Sb (3.44), O (2.54), E 1 (2.53//0.5;0.0;0.75), E 2 (1.49//0.5;0;0.88), E 3(1.34//0.28; – 0.28;0.06). Ca_4Sb: 59 irreducible k-points, Ca 1 (3.57), Ca 2 (3.43), Sb (3.44), E 1 (1.48//0;0;0.5), E 2 (2.42//0.5;0;0.75), E 3 (1.46//0;0;0).
[38] T. A. Albright, J. K. Burdett, M. H. Whangbo, *Orbital Interactions in Chemistry*, Wiley, New York, **1985**.
[39] K. Fukui, *Science* **1982**, *218*, 747.
[40] Ba_3Ge_4: 59 irreducible k-points, Ba 1 (4.95), Ba 2 (4.60), Ge (2.67). Ba_3Ge_4O: 59 irreducible k-points, Ba 1 (4.26), Ba 2 (4.53), Ge (2.74), O (2.53), E 1 (1.59//0.25;0.25;0.25), E 2 (1.37//0.21;0.06;0.11). $Ba_{10}Ge_7$: 70 irreducible k-points, Ba 1 (4.26), Ba 2 (4.52), Ba 3 (3.91), Ba 4 (4.70), Ge 1 (2.61), Ge 2 (3.26), E 1 (3.02//0.33;0.67;0.0), E 2 (1.57//0.30;0.15;0). $Ba_{10}Ge_7O_3$: 70 irreducible k-

points, Ba 1 (3.93), Ba 2 (4.61), Ba 3 (3.42), Ba 4 (4.80), Ge 1 (2.67), Ge 2 (3.75), O (2.18), E 1 (3.20//0.33;0.67;0.0), E 2 (1.75//0.30;0.15;0.5), E 3 (1.40//0.38;0.45;0.5), E 3 (1.37//0;0;0).

[41] In Ba_3Ge_4X one finds a split position for X, which is in accord with a tetragonal disordered acetylide anion C_2^{2-}; H. G. von Schnering, personal communication. Naturally, the ELF distribution based on Ba_3Ge_4 also allows a C_2^{2-}. As expected it does not give any hints of an atom distribution of lower symmetry.

[42] A. Simon, H. G. von Schnering, H. Schäfer, *Z. Anorg. Allg. Chem. C* **1967**, *355*, 295; *ibid.* **1967**, *355*, 311; H. Imoto, A. Simon, *Inorg. Chem.* **1982**, *21*, 308.

[43] F. Böttcher, A. Simon, R. K. Kremer, H. Buchkremer-Hermans, J. K. Cockcroft, *Z. Anorg. Allg. Chem. C* **1991**, *598*, 25; A. Simon, F. Böttcher, J. K. Cockcroft, *Angew. Chem.* **1991**, *103*, 79; *Angew. Chem. Int. Ed. Engl.* **1991**, *30*, 101.

[44] CaH_2: 45 irreducible k-points, Ca (3.06), H 1 (1.70), H 2 (2.01), E 1 (1.96// − 0.27;0.5;0), E 2 (1.75//0.5;0;0), E 3 (1.64//0;0;0.28). "CaH": 45 irreducible k-points, Ca (3.27), H 2 (1.81), E 1 (1.99//0.38;0.25;0.43), E 2 (1.56//0.18; − 0.25;0.29), E 3 (1.53//0.12;0.25;0.45), E 4 (1.43//0.49; − 0.25;0.43). "Ca": 45 irreducible k-points, Ca (3.79), E 1 (1.67//0.48; − 0.25;0.30).

[45] SrSi: 95 irreducible k-points, Sr 1 (4.49), Sr 2 (3.81), Sr 3 (3.81), Sr 4 (4.30), Sr 5 (4.21), Si 1 (2.60), Si 2 (2.60), Si 3 (2.60), E 1 (1.58// − 0.23;0;0.5), E 2 (1.47//0.5;0;0), E 3 (1.53//0;0;0.28), E 4 (1.45// − 0.35;0.0;0.26). SrSiO: 95 irreducible k-points, Sr 1 (4.53), Sr 2 (3.17), Sr 3 (3.38), Sr 4 (4.05), Sr 5 (4.26), Si 1 (2.63), Si 2 (2.63), Si 3 (2.64), O (2.17//0.5;0;0), E 1 (2.08// − 0.18;0;0.5), E 2 (1.72//0;0;0.29), E 3 (1.56//0.15; − 0.5;0.25), E 4 (1.41//0.40; − 0.28;0.07), E 5 (1.41//0.33;0.13; − 0.11).

[46] W. Gerlach, *Z. Phys.* **1922**, *9*, 184; W. Primak, H. Kaufmann, R. Ward, *J. Am. Chem. Soc.* **1948**, *70*, 2043.

[47] H. D. Megaw, *Proc. Phys. Soc. London* **1948**, *58*, 133; J. Hutton, R. J. Nelmes, *Acta Crystallogr.* **1981**, *38*, 916.

[48] A. Currao, R. Nesper, unpublished results.

[49] R. Hoffmann, *J. Chem. Phys.* **1963**, *39*, 1397; R. Hoffmann, *Solids and Surfaces: A Chemist's View of Bonding in Extended Structures*, VCH, Weinheim/New York, **1988**; Program EHMACC based on R. Hoffmann, W. N. Lipscomb, *J. Chem. Phys.* **1962**, *36*, 2179; M.-H. Whangbo, R. Hoffmann, R. B. Woodward, *Proc. R. Soc. London* **1979**, *A366*, 23.

[50] The extended Hückel calculation was performed (without preceeding charge iterations) with the following atom parameters and on the basis of the crystal structure: Sr: $H_{ii}(5s) = -6.62$ eV, $z(5s) = 1.214$; $H_{ii}(5p) = -3.92$ eV, $z(5p) = 1.214$; Si: $H_{ii}(3s) = -17.30$ eV, $z(3s) = 1.383$; $H_{ii}(3p) = -9.20$ eV, $z(3p) = 1.383$.

[51] According to general findings, EH calculations overestimate and LMTO calculations underestimate the magnitude of band gaps. If neither of the two methods shows a gap the probability for a metallic system is very high.

[52] D. H. Berry, *J. Am. Chem. Soc.* **1994**, *116*, 177; A. F. Hollemann, E. Wiberg, N. Wiberg, *Lehrbuch der Anorganischen Chemie*, 101st ed., de Gruyter, Berlin, **1995**, pp. 885 ff.

[53] C. Maerker, M. Kaupp, P. von Ragué Schleyer, in *Organosilicon Chemistry Vol. II, From Molecules to Materials* (Eds.: N. Auner, P. Weis), VCH, Weinheim, **1995**, pp. 329 ff.

[54] A. Currao, J. Curda, R. Nesper, *Z. Anorg. Allg. Chem. C* **1996**, *622*, 85.

[55] A. Currao, Dissertation No. 11747, ETH Zürich, **1996**.

[56] R. Janoschek, *J. Inorg. Organomet. Polym.* **1993**, *3*, 277.